Magnetized Binary Neutron Star Merger Simulations

Kenta Kiuchi,[1] Koutarou Kyutoku,[2] Kenta Hotokezaka,[3] Yuichiro Sekiguchi,[1] and Masaru Shibata[1]

[1]*Yukawa Institute for Theoretical Physics, Kyoto University, Kyoto, 606-8502, Japan*

[2]*Theory Center, Institute of Particles and Nuclear studies, KEK, Tsukuba, Ibaraki, 305-0801, Japan*

[3]*Department of Physics, Kyoto University, Kyoto, 606-8502, Japan*

Abstract. We perform general relativistic magnetized binary neutron star (BNS) merger simulations. Our aim of this study is to explore a magnetic field amplification mechanism in BNS mergers and a final configuration of amplified magnetic field. Our main findings are that the magnetic field is amplified by the Kelvin Helmholtz instability at the merger and magneto rotational instability inside an accretion torus, which is formed after a remnant massive neutron star collapses to a black hole. The saturation energy of magnetic field is several percents of a kinetic energy of the accretion torus. Our result suggests that a long-term simulation with a high resolution is mandatory to explore the final state of magnetized BNS merger.

1. Introduction

Observationally, it is suggested that neutron stars have a magnetic field of canonical strength of 10^{11-13} G. Among them, there is a special class called magnetars, which have an ultra strong magnetic field of 10^{14-15} G.

Double neutron star binary is one of most promising source of gravitational waves (GWs). Next generation GW detectors such as KAGRA, advanced LIGO, and advanced VIRGO (Abadie et al. 2010) could detect mergers of binary neutron stars (BNS) with ~ 1–100 events per year (Kalogera et al. 2007). Therefore, it is natural to ask a question what the role of magnetic field is during the mergers of BNSs. There are four candidates of magnetic field amplification process in BNS mergers; the Kelvin Helmholtz (KH) instability developed in the shear layer when the two stars come into contact, the magneto rotational instability (MRI) (Balbus & Hawley 1998) inside remnant massive neutron stars (RMNS) formed after the merger and/or massive tori formed after a black hole (BH) formation, compression, and magnetic winding. If these amplification processes work and strong magnetic field could be produced, it would change the structure of the RMNSs or proceed the angular momentum transport inside the RMNSs and/or massive accretion tori around the BH. Motivated by these facts, a number of simulation of magnetized BNS has been done so far in the framework of Newtonian gravity and general relativity (Price & Rosswog 2006).

However, it is hard to say these previous works have drawn a decisive conclusion for magnetic amplification in BNS because the simulations have been done on somewhat limited models such as the equation of states (EOS) and/or magnetic field configuration and strength. In particular, a shortwave-length mode is essential for the KH instability and MRI mentioned above and the grid width adopted in these simulations is insufficient to resolve them. Therefore, in this paper, we report magnetized BNS simulations in Numerical Relativity, in which the systematic study for the magnetic field strength as well as the grid resolution is done and the neutron star is modeled with a different EOS used in the previous works. Note that in the previous works the Gamma-law EOS with the polytropic index being is unity is always adopted. However, the mass-radius relation with this EOS is substantially different from the nuclear-theory based EOSs. Throughout this paper, we adopt c=G=1 unit with c and G being the speed of light and the gravitational constant.

2. Numerical setup

The numerical code for general relativistic magnetosphere dynamical (GRMHD) simulation used in this paper has been developed in Kiuchi et al. (2012). The Einstein solver is based on the Baumgarte–Shapiro–Shibata–Nakamura-puncture formulation (Shibata & Nakamura 1995) with a fourth-order accuracy both in time and space. We implement a high resolution central scheme together with a third order reconstruction scheme to solve the GRMHD equations (Kurganov 2000). To resolve a gravitational wave as well as a neutron star and BH formed after the merger, we implement the fixed mesh refinement technique in which the divergence free condition and magnetic flux conservation are simultaneously satisfied (Balsara & Spicer 1999). The resolution of a parent refinement domain is twice larger than that of a child domain and a total refinement level is seven in all the models.

The recent observation of PSR J1614-2230 suggests that a maximum mass of spherical cold neutron star should be greater than about $2M_\odot$ (Demorest et al. 2010). This constraint implies that a RMNS would be formed after BNS of the canonical mass $2.7 - 2.8M_\odot$ because the remnant neutron star has a rapid and strong differential rotation in general. Therefore, one has to model a neutron star with the EOS which passes this observational constraint. In this paper, we adopt the EOS called H4 (Gledenning & Moszkowski 1991) based on the relativistic mean field theory together with the hyperon effect. The maximum mass of a spherical neutron star with this EOS is $2.03M_\odot$. In Table 1, we summarize the models simulated in this paper. We select an equal mass binary of canonical mass $2.7 - 2.8M_\odot$ and vary the maximum magnetic field strength from 3.33×10^{14} G to 10^{15} G. Following the previous works (Price & Rosswog 2006), the purely poloidal magnetic field is confined inside the star. Quasi equilibrium configuration of binary neutron stars is used as an initial condition, in which we assume a conformal flatness. The simple copy boundary condition for the magnetic field and outgoing boundary condition for the gravitational waves are adopted.

3. Numerical results

Left panel of Fig. 1 plots the evolution of maximum rest-mass density field. This figure shows RMNSs are formed after the merger $t - t_{\mathrm{merge}} = 0$ irrespective of the models

Model	$m_1 - m_2$ [$M_\odot$]	$|B|_{max}$ [G]	Δx_{min} [m]	$2R_{NS}/\Delta x_{min}$	L [km]
M135C15	1.35-1.35	10^{15}	230	100	2264
M135C14	1.35-1.35	3.33×10^{14}	230	100	2264
M14C15	1.4-1.4	10^{15}	223	100	2300
M14C15M	1.4-1.4	10^{15}	279	80	2322
M14C15L	1.4-1.4	10^{15}	372	60	2357
M14C14	1.4-1.4	3.33×10^{14}	223	100	2300

Table 1.   Model name, gravitational mass of each neutron star in isolation, maximum magnetic field strength, and the finest grid resolution. The last two column is a coordinate diameter of neutron star divided by the grid resolution and location of the outer boundary.

because one can find a gradual increase of the maximum density with oscillations for $t - t_{merger} \geq 0$. Then, the density exhibits the blow-up implying the formation of a BH. This BH formation is triggered by the angular momentum loss due to the gravitational wave emission as well as the hydrodynamical angular momentum transport due to the non-axisymmetric structure of the RMNS. The point is that for the massive model such as M14C15 and M14C14 the density evolution is almost perfectly overlapped, which means that the magnetic field does not play a substantial role in the inspiral phase and the RMNS phase. On the other hand, for the less massive model M135C15 and M135C14, the lifetime of the RMNS is significantly different, i.e., the BH forms at $t-t_{merger} \approx 20$ ms for M135C14 and ≈ 60 ms for M135C15. This indicates the amplified magnetic field affects the evolution of the RMNS. As mentioned in Introduction, the primary amplification mechanism of magnetic field at the merger is the KH instability. When the two stars come into contact, the surface of the two stars forms a shear layer in which the KH instability develops. The poloidal magnetic field lines are curled by the vortexes due to the KH instability and strong toroidal magnetic field is generated as a result. Right panel of Fig. 1 is a density weighted vorticity at the merger on the equatorial plane, from which one can infer that this amplification mechanism would work in the magnetized BNS merger.

Figure 2 plots the evolution of poloidal and toroidal components of magnetic field energy in all the models. Irrespective of the models, both components remain approximately constant value before the merger. Then, the toroidal component as well as the poloidal component suddenly increases at the merger. The former is due to the KH instability as mentioned above. The later amplification originates from the compression because the star is significantly compressed at the merger as shown in Fig. 1. Assuming the magnetic flux conservation, the poloidal field increase should be proportional to $\rho^{2/3}$ with ρ being the rest-mass density. We find this indeed happens in the poloidal component increase. The amplified toroidal magnetic field overtakes the poloidal field just after the merger. Therefore, the RMNSs have a dominant toroidal field. Because the RMNSs have a rapid and strong differential rotation, the magnetic winding is the amplification process during the RMNS phase. Figure 2 clearly shows that this mechanism indeed works during this phase and we find that the toroidal field grows as $\sim B_P \Omega t$ with B_P and Ω being the poloidal field and angular velocity. Note that in the RMNS phase MRI would turn on as well. However, the MRI wavelength for the maximum growing mode is $6 \times 10^3 (B_P/10^{14}\mathrm{G})(\rho/10^{15}\mathrm{g/cm^3})^{-1/2}(\Omega/10^3\mathrm{rad/s})^{-1}$ cm and a required grid resolution is $\sim 60 - 70$ cm to cover the wavelength with $8 - 10$ grid points.
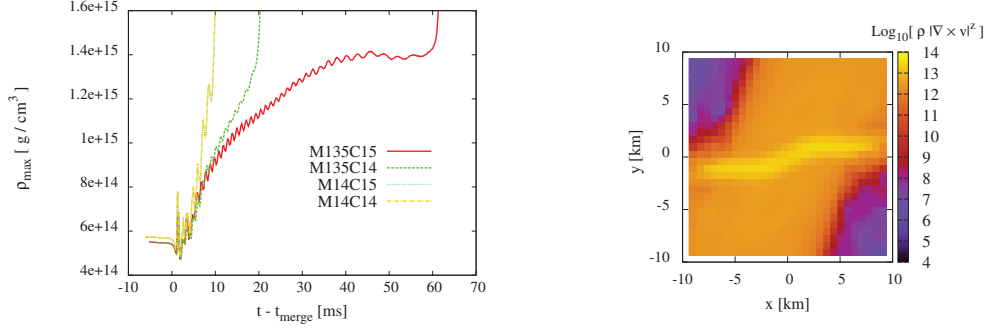
Figure 1. (Left) Maximum rest-mass density field as a function of $t - t_{\mathrm{merge}}$. (Right) Density weighted vorticity on the equatorial plane at $t - t_{\mathrm{merge}} \approx 0.6$ ms for model M14C15. t_{merge} is a merger time.

Simulation with this resolution is infeasible with a current computational resource (see also Table 1). In model M135C15, the amplified toroidal magnetic field produces a strong magnetic pressure and play a substantial role to sustain the RMNS. This leads a very long-lived RMNS as discussed above. On the other hand, in model M135C14, the magnetic field is not significantly amplified and then, the RMNS collapses to the BH within about 20 ms. In model M14C15 and M14C14, the contribution of the magnetic pressure is insufficient to sustain the star because the RMNS is fairly massive.

The vertical dotted lines in Fig. 2 indicates a formation of apparent horizon, i.e., BH formation. Soon after the BH formation, an eager accretion onto the BH starts and most fluid elements are swallowed into the BH. Fluid elements who have an sufficient specific angular momentum to escape from the capture by the BH survive as an accretion torus and we find that its rest mass is $\sim 10^{-1} M_\odot$ for model M135C15, $\sim 5\times10^{-2} M_\odot$ for model M135C14, and $\sim 2 \times 10^{-2} M_\odot$ for model M14C15 and M14C14 at 30 ms after the BH formation. Note that the RMNS lifetime is quite long for model M135C15 as discussed above and angular momentum transport works in this phase. This results in a massive accretion torus formation. Because of the rapid accretion, the magnetic field energy rapidly decreases after the BH formation. Then, both poloidal and toroidal components exhibit the exponential growth, irrespective of the models except M135C15. Magnetic field grows inside the accretion torus and we infer that the MRI drives this exponential growth. The typical density field and angular velocity inside the torus are 10^{11-12} g/cm^3 and 10^{2-3} rad/s. The wavelength of the maximum growing mode is $\sim 10^5$ cm$(\rho/10^{12}$g/cm$^3)^{-1/2}(B^z/10^{14}$G$)(\Omega/10^3$rad/s$)^{-1}$. E-folding time is 5.4 ms for model M135C14, and 7.7 ms for model M14C15 and M14C14. Because the grid resolution is $\sim 2 \times 10^4$ cm for the highest resolution case and the e-folding time of the maximum growing mode should be ~ 1ms for $\Omega = 10^3$ rad/s, we consider that the maximum growing mode cannot be resolved in our simulations. Nevertheless, the growing mode is likely to be resolved with the highest resolution case. In other words, the long wavelength mode than the maximum growing mode is resolved and the growth rate of this mode is smaller than that for the maximum growing mode $\sim \Omega$ (Balbus & Hawley 1998). In the left-bottom panel, we plot the result with a high, medium, and low resolution case (see also Table 1). With the low resolution, one can find that noth-
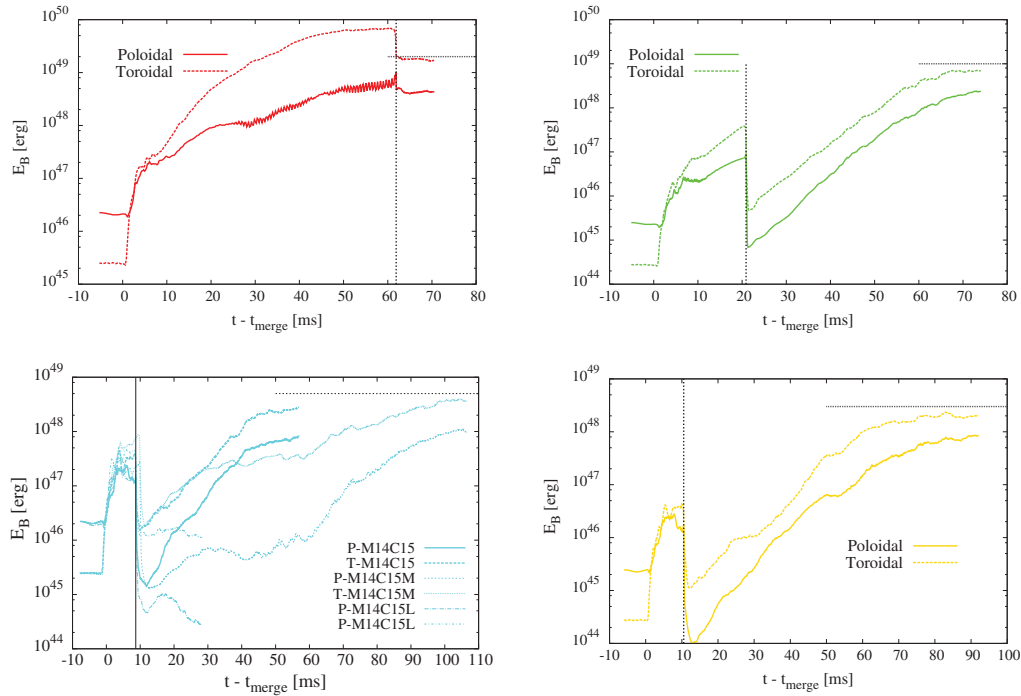
Figure 2. Poloidal and toroidal magnetic field energy as a function of time for model M135C15 (left-top), M135C14 (right-top), M14C15 (left-bottom), and M14C14 (right-bottom). The vertical dotted lines are the formation time of apparent horizon and horizontal dashed lines a saturation energy of the magnetic field (see the text in details). For model M14C15, P and T mean poloidal and toroidal field energy, respectively.

ing happens because the wavelength of the unstable mode is too long and the growth rate is too small. With the medium resolution, the magnetic energy still shows the exponential growth, but its growth rate is smaller than the high resolution run. These findings support our conjecture that not the maximum growing mode, but the growing mode is resolved in our simulation. Notable point is that the magnetic field energy E_{B} saturates at several tens of milliseconds after the black hole formation and a saturation level does not depend on the grid resolution. We evaluate the kinetic energy E_{kin} and thermal energy E_{thr} of the accretion torus and find $E_{\mathrm{B}}/E_{\mathrm{kin}} \approx 2 - 5\%$ and E_{B} and E_{thr} are almost comparable.

4.　Summary and future perspectives

We performed magnetized binary neutron star merger simulation in the framework of Numerical Relativity. The BNS is modeled so as to pass through the observational constraint for the maximum mass and have a canonical mass as well. We vary the magnetic field strength as well as the grid resolution of the numerical simulation to explore the

magnetic field amplification mechanism. With our choice of the equation of state, the black hole surrounded by the strongly magnetized accretion torus is a canonical outcome of BNS merger and the magnetic field is amplified by the KH instability at the merger and MRI inside the accretion torus. However, the grid resolution is still insufficient to resolve the maximum growing mode of MRI and we don't find an ordered magnetic field line in the end of the simulation. This implies that a longer simulation, e.g., $\sim$ 100ms, with a higher resolution, e.g., $\Delta x_{min} \sim 100$ m, is mandatory. The growth rate of the magnetic field due to the KH instability is smaller than that reported in Price & Rosswog (2006). If we could find a larger growth rate in the high resolution simulation, a new born MNS would have a stronger magnetic field than the MNSs reported in this paper and the MRI could be resolved in a MNS phase. The amplified magnetic field due to the MRI inside the torus will proceed an accretion. The high resolution run will give an answer to this question. Moreover, we should do the systematic study for the equation of states because the EOS in this work is nothing but a representative model. We plan to do such a simulation on the K computer.

References

Abadie, J., et al. 2010, Nucl. Instrum. Methods Phys. Res. Sect., A624, 223; Accadia, T. et al. 2011, CQG, 28, 025005; Kuroda, K., et al. 2010, CQG, 27, 084004

Balbus, S. A., and Hawley, J. F. 1998, Rev. Mod. Phys., 70, 1

Balsara, D., and Spicer, D. 1999, J. Comp. Phys., 149, 270

Demorest, P., Pennucci, T., Ransom, S., Roberts, M., and Hessels, J. 2010, Natur, 467, 1081

Glendenning, N. K., and Moszkowski, S. A. 1991, Phys. Rev. Lett., 67, 2414

Kalogera, V., et al. 2007, Phys. Rep., 442, 75

Kiuchi, K., Kyutoku, K., and Shibata, M. 2012, Phys. Rev. D, 86, 064008

Kurganov, A., and Tadmor, E. 2000, J. Comput. Phys., 160 214

Price, D., and Rosswog, S. 2006, Science, 312 719; Liu, Y. T., Shapiro, S. L., Etienne, Z. B., and Taniguchi, K. 2008, Phys. Rev. D, 78, 024012; Anderson, M., et al. 2008, Phys. Rev. Lett., 100, 191101; Giacomazzo, B., Rezzolla, L., and Baiotti, L. 2011, Phys. Rev. D, 83, 044014.

Shibata, M., and Nakamura, T. 1995, Phys. Rev. D, 52, 5428; Baumgarte, T. W., and Shapiro, S. L. 1999, Phys. Rev. D, 59, 024007; Campanelli, M., Lousto, C. O., Marronetti, P., and Zlochower, Y. 2006, Phys. Rev. Lett., 96, 111101; Baker, J. G., Centrella, J., Choi, D.-I., Koppitz, M., and van Meter, J. 2006, Phys. Rev. Lett., 96, 111102